SERBIAN JOURNAL OF ELECTRICAL ENGINEERING
Vol. 22, No. 2, June 2025, 267-279

UDC: 621.396.674:004.94 **DOI: https://doi.org/10.2298/SJEE2502265A**

Original scientific paper

UWB Slot-Loaded Antipodal Vivaldi Antenna for Through-the-Wall Radar Imaging (TWRI) Applications

Sajjad Ahmed[1,2], Ariffuddin Joret[2], Norshidah Katiran[2], Muhammad Inam Abbasi[3], Nuramin Fitri Aminuddin[2]

Abstract: The study presents an Ultra-Wideband Slot-loaded Antipodal Vivaldi Antenna (SL-AVA) designed for through-the-wall radar imaging (TWRI) applications. The antenna incorporates rectangular slots of varying lengths and widths, effectively extending its electrical length and suppressing surface waves. These variable-length slots play a crucial role in enhancing overall performance by improving bandwidth, impedance matching, and radiation characteristics. Fabricated on a Rogers 5880 substrate with dimensions of 60.50 × 66.10 mm², the SL-AVA operates efficiently across a wide frequency range of 3 GHz to 10 GHz. It achieves a peak gain of 11 dBi. Experimental fabrication and testing validate the SL-AVA antenna's characteristics, including compact size, high gain, ultra-wide bandwidth, and directional radiation, making it an excellent choice for TWRI applications.

Keywords: Slot-loaded Antipodal Vivaldi Antenna (SL-AVA), TWRI, UWB.

1 Introduction

In recent times, the emergence of through-wall radar imaging (TWRI) technology has drawn considerable interest due to its versatile applications across domains. From search and rescue operations to law enforcement and military tasks, TWRI employs [1 − 3] radar waves to penetrate solid barriers like walls, revealing vital information about concealed objects and individuals.

[1]Faculty of Engineering, The University of Larkano, Larkana, Sindh, Pakistan, sajjadbhatti_35@hotmail.com, https://orcid.org/0009-0001-9060-2114
[2]Faculty of Electrical and Electronic Engineering, Universiti Tun Hussein Onn Malaysia, Johor, Malaysia, ariff@uthm.edu.my, https://orcid.org/0000-0002-3160-9674;
norshida@uthm.edu.my, https://orcid.org/0000-0002-5721-2413;
he200011@siswa.uthm.edu.my, https://orcid.org/0000-0002-9816-5238
[3]Fakulti Teknologi Dan Kejuruteraan Elektronik Dan Komputer (FTKEK), Universiti Teknikal Malaysia, Durian Tunggal, Melaka Malaysia, inamabbasi@utem.edu.my, https://orcid.org/0000-0002-3127-4923

Colour versions of the one or more of the figures in this paper are available online at https://sjee.ftn.kg.ac.rs

This capability has transformed our perception and interaction with the environment, establishing TWRI as an essential tool in various scenarios. The antenna is a crucial component in TWRI, transmitting and receiving electromagnetic signals to collect vital data from obscured environments [4]. The performance and reliability of the antenna play a critical role in determining image resolution, sharpness, and penetration depth, which are vital for accurate and detailed TWR. The AVA stands out as a strong candidate for TWRI applications due to its outstanding characteristics, making it particularly suitable for scenarios that demand high-resolution imaging and precise target detection, even in the presence of physical obstructions [5]. Therefore, developing an efficient antenna for TWRI is crucial for outstanding performance and accuracy.

The AVA is a distinct design known for its ultra-wide bandwidth and directional radiation characteristics [6], making it ideal for applications such as TWRI. Its tapered slot structure, shaped similarly to a flared horn, facilitates efficient radiation and propagation of electromagnetic waves across a broad frequency range. The antenna's carefully optimized geometry contributes to achieving high gain with minimal sidelobe interference. Thanks to its broad operating bandwidth, the AVA antenna supports operation across multiple frequency bands, offering flexibility in frequency selection and multi-band functionality. UWB technology enhances the AVA antenna's performance and versatility, offering wide frequency coverage, high data rates, precise imaging capabilities, improved signal penetration, and reduced interference [7 – 8].

This study presents a UWB antenna design using the SL-AVA configuration for (TWRI) applications. The antenna structure integrates multiple rectangular slots of variable lengths and uniform width (1 mm) symmetrically etched on both flares to enhance bandwidth and improve radiation characteristics. The model is fabricated on a Rogers RT/Duroid 5880 substrate, characterized by a dielectric constant of $\varepsilon_r = 2.2$ and a substrate thickness of 1.58 mm. The proposed antenna exhibits a stable radiation pattern across the operating frequency band, maintains consistent gain, and achieves low return loss (S11 < –10 dB) and voltage standing wave ratio (VSWR < 2), making it suitable for high-resolution TWRI applications

2 Slot-Loaded Antipodal Vivaldi Antenna (SL-AVA) Design

The SL-AVA antenna is fabricated on a Rogers RT/Duroid 5880 substrate, featuring a dielectric constant (ε_r) of 2.2 and a substrate thickness of 1.58 mm. The slotted geometry of the radiating patch contributes to improved bandwidth and radiation properties. A microstrip feed line with a 50 Ω impedance and a width (w_C) of 4.58 mm is employed to ensure proper matching over the desired frequency range. Rogers 5880 is specifically selected due to its low dielectric loss tangent ($\tan\delta \approx 0.0009$), which supports high radiation efficiency and gain [9]. The SL-AVA structure incorporates a pair of identical elliptic arcs, as previously validated in [10 – 12], to improve current distribution and facilitate UWB operation. Theoretically, the Vivaldi antenna is designed to operate with an unlimited upper frequency range, its lower frequency threshold is generally governed by the width of the structure and the value of the effective dielectric constant (ε_{eff}) as represented in (1) and (2). The dielectric value of the substrate is represented by ε_r and ε_{eff} is an effective dielectric value of the substrate with air equal to 1 and varying with c, the speed of light:

$$f_{\min} = \frac{\mathrm{c}}{2w\sqrt{\varepsilon_{\mathrm{eff}}}}, \tag{1}$$

$$\varepsilon_{\mathrm{eff}} = \frac{\varepsilon_{\mathrm{r}}+1}{2} + \frac{\varepsilon_{\mathrm{r}}-1}{2}\left(1+\frac{12h}{w}\right)^{-1/2}, \tag{2}$$

$$z_o = \frac{60}{\sqrt{\varepsilon_{\mathrm{eff}}}}\ln\left(\frac{8h}{w}+\frac{w}{4\mathrm{h}}\right), \quad \mathrm{for}\left(\frac{w}{h}\right)<1, \tag{3}$$

$$z_o = \frac{120\pi}{\sqrt{\varepsilon_{\mathrm{eff}}}\left[\frac{w}{h}+1.393+\frac{2}{3}\ln\left(\frac{w}{h}+1.444\right)\right]}, \quad \mathrm{for}\left(\frac{w}{h}\right)\geq 1. \tag{4}$$

The antenna is built around two core components, the feed line and the flared radiators. To achieve better performance, the SL-AVA design includes a slot-based structure [13 – 15]. Variable-length slots in SL-AVA significantly enhance performance by improving bandwidth, impedance matching, and radiation characteristics. Fixed-length slots, on the other hand, may limit the antenna's efficiency, leading to narrowband operation and poor radiation properties. The slots help fine-tune the antenna's impedance, reducing reflection losses and improving input return loss. They also broaden the operational bandwidth, enabling UWB applications. The slot structure minimizes surface wave propagation, reducing losses and improving radiation efficiency. The precise arrangement and dimensions of the slots, such as the antenna incorporates 17 rectangular slots of different lengths but a constant width of 1 mm, which ensures stable radiation characteristics throughout the operational band. Additionally, the slots enhance gain by directing the radiated energy more efficiently. The Parameter Sweeping technique is utilized to optimize the dimensions of SL-AVA by systematically varying parameters like length, slot width, and feeding structure dimensions within a specified range, while keeping others constant, to determine their impact on the antenna's performance.

Varying slots in SL-AVA offer several advantages, including enhanced bandwidth, improved radiation patterns, and gain improvement. They also help in reducing return loss and minimizing cross-polarization effects. However, these benefits come with challenges such as increased design complexity, manufacturing difficulties, and potential bandwidth trade-offs. Proper optimization is essential to balance these advantages and disadvantages effectively. The antenna was designed and optimized using CST Microwave Studio®, a robust tool for electromagnetic simulation and analysis. This software facilitates the modeling, evaluation, and refinement of diverse electromagnetic structures. For the proposed antenna, dimensional parameters (in millimeters) were fine-tuned, as summarized in **Table 1**. Furthermore, the antenna's physical configuration is illustrated in Fig. 1, where Fig. 1a shows the version without slots and Fig. 1b displays the slotted configuration

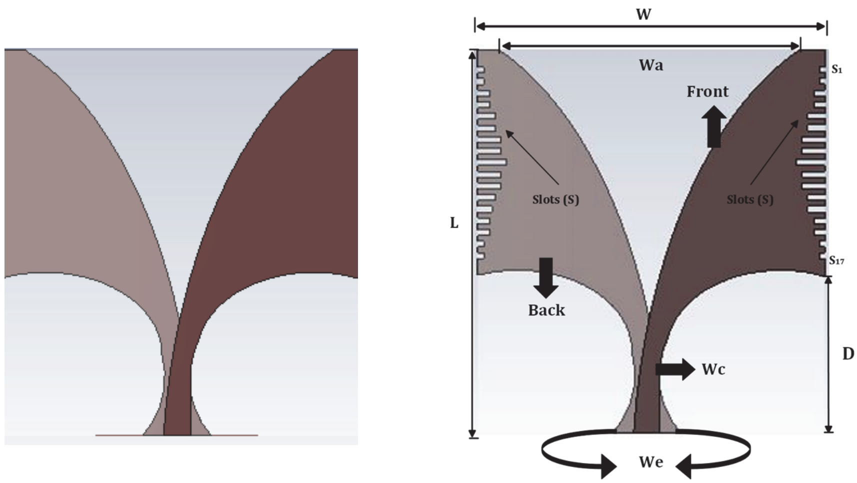

(a) (b)

Fig. 1 – *SL-AVA antenna geometric layout:* (a) *Without slots;* (b) *With slots.*

Table 1

Dimensions of SL-AVA.

Parameters	Values (mm)	Parameters	Values (mm)
w	60.50	$S_L (S_3 - S_4)$	2
L	66.10	$S_L (S_5 - S_6)$	3
D	27	$S_L (S_7 - S_8)$	4
wa	52.50	$S_L(S_9)$	5
wc	4.58	$S_L (S_{10} - S_{11})$	4
we	11.80	$S_L (S_{12} - S_{13})$	3
$S_W (S_1 - S_{17})$	1	$S_L (S_{14} - S_{15})$	2
$S_L (S_1 - S_2)$	1	$S_L (S_{16} - S_{17})$	1

3 Simulation Results

The simulated far-field directivity response of the SL-AVA antenna within the 3 GHz to 10 GHz range is illustrated in Fig. 2, using CST Microwave Studio®. These radiation patterns provide detailed insights into the spatial energy distribution of the antenna at selected frequencies. To evaluate the directional performance of the antenna, key radiation features including the magnitude and direction of the main lobe, side lobe levels (SLL), and beam width are extracted. The main lobe indicates the direction of maximum radiation, whereas the side lobes correspond to secondary radiation lobes with lower intensity. Analysis of the directivity plots across the UWB range reveals frequency-dependent variations in beam direction, radiation strength, and side lobe formation, offering a comprehensive understanding of the antenna's far-field behavior and its suitability for TWRI applications.

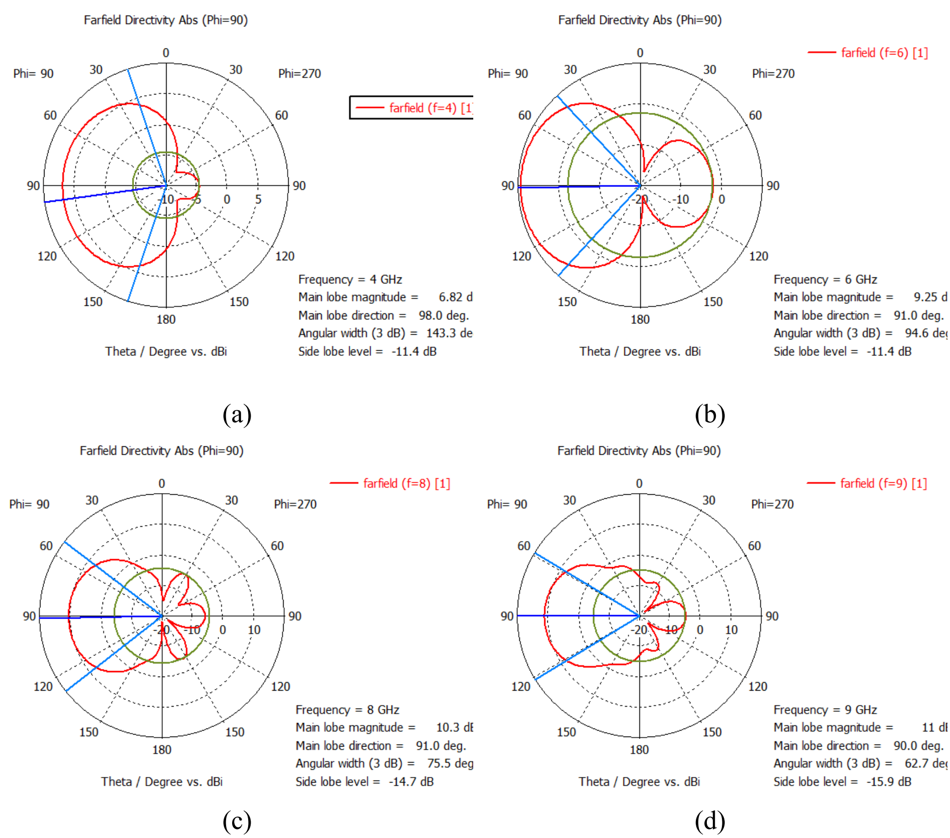

Fig. 2 – *Far-field directivity plots of SL-AVA:*
(a) 4 GHz; (b) 6 GHz; (c) 8 GHz; (d) 9 GHz.

As shown in Fig. 3, the SL-AVA antenna's 3D far-field radiation patterns, spanning frequencies from 3 GHz to 10 GHz, were simulated using CST Microwave Studio®. These 3D visualizations deliver a more complete representation of the antenna's directional radiation properties compared to 2D plots, enabling detailed observation of both the intensity and directionality of the radiated electromagnetic fields. These patterns emphasize the gain distribution at various frequencies, which is a key parameter reflecting the antenna's capability to direct radiated power effectively. Antenna gain, as visualized in the 3D patterns, quantifies the ratio of power emitted in a particular path to that of an ideal isotropic radiator. This directional gain is critical in evaluating the antenna's performance in focusing energy toward desired directions, particularly in TWRI applications where directional radiation enhances target resolution and detection accuracy.

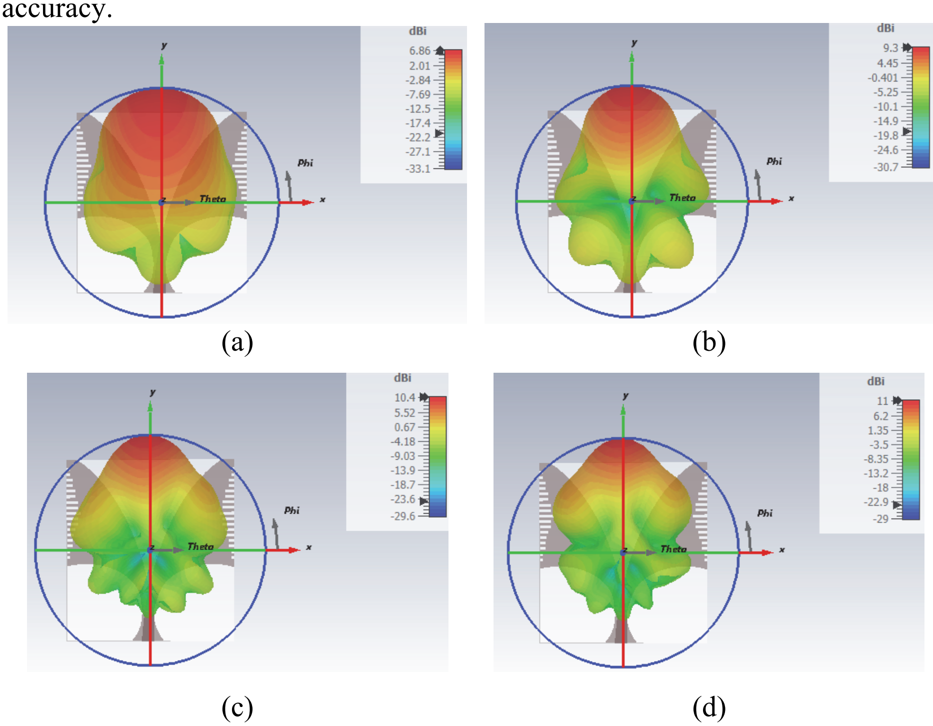

Fig. 3 – *Three-dimensional far-field radiation pattern of SL-AVA:*
(a) 4 GHz; (b) 6 GHz; (c) 8 GHz; (d) 9 GHz.

The presented 3D simulations facilitate an in-depth analysis of the SL-AVA antenna's behavior across the UWB spectrum. Variations in beam shape, direction, and intensity across frequencies are examined to assess radiation symmetry and concentration. These insights are instrumental for optimizing the antenna's structural parameters, ensuring high gain, improved directivity, and minimal radiation leakage, thereby enhancing its operational efficiency in wideband imaging and sensing scenarios.

The simulated gain characteristics of the SL-AVA antenna, with and without slots, are depicted in Fig. 4 for the 3–10 GHz UWB band. A notable rise in gain is observed within the 6–10 GHz frequency range, with the peak simulated gain occurring at 9 GHz when slots are incorporated into the antenna design, reaching approximately 11 dBi. In contrast, the gain of the antenna without slots remains lower compared to the slotted design, despite showing an increase in the higher frequency range. The peak simulated gain for the design without slots occurs at 7 GHz, reaching approximately 9.2 dBi. These findings highlight the significant impact of incorporating slots in enhancing the antenna's gain performance, particularly at higher frequencies. Fig. 5 presents a comparison of the simulated reflection coefficients (S11) for the SL-AVA antenna with and without slots across the UWB frequency range. The results indicate that the slotted design maintains an acceptable reflection coefficient, remaining below the -10 dB threshold throughout the entire UWB band. In contrast, the design without slots only not meet this criterion within a limited frequency spectrum, specifically between 3.8 GHz and 4.4 GHz. This demonstrates the effectiveness of the slotted design in achieving better impedance matching across the UWB spectrum.

Table 2 presents a comparison of antenna gain across the UWB frequency range for both slotted and non-slotted configurations. The gain of the antenna without slots varies between 3 dBi and 9.2 dBi, whereas the slotted antenna exhibits an enhanced gain ranging from 3.4 dBi to 11 dBi. This improvement suggests that the introduction of slots effectively modifies the antenna's current distribution, leading to enhanced radiation efficiency and improved directionality. The higher gain values in the slotted design indicate a better concentration of radiated power, which is advantageous for applications requiring stronger and more focused signal propagation.

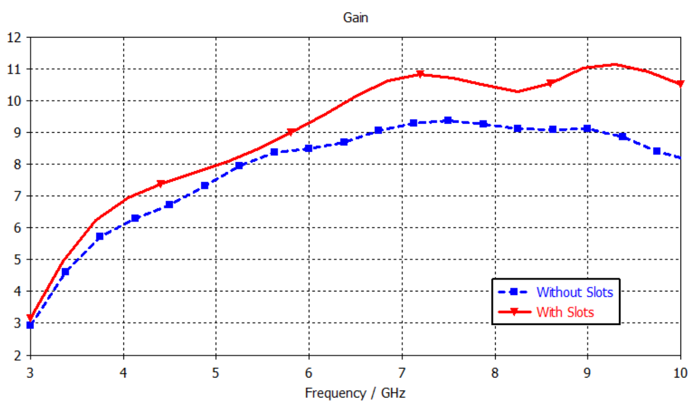

Fig. 4 – *Simulated gain of SL-AVA with slots and without slots.*

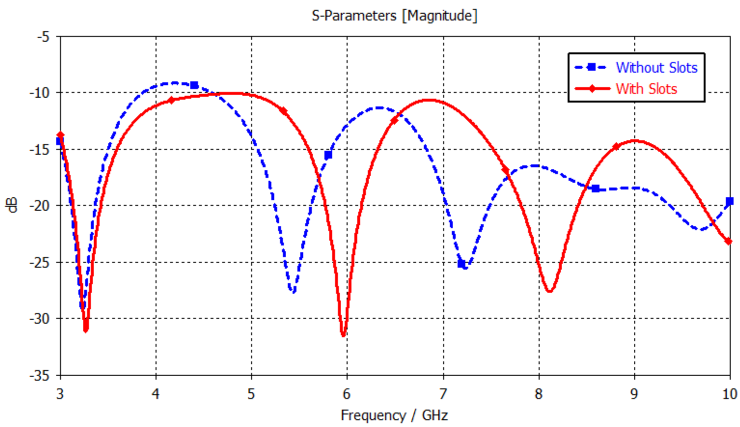

Fig. 5 – *Simulated S_{11} of SL-AVA with slots and without slots.*

Table 2
Gain of SL-AVA with slots and without slots.

Frequency	Gain (dBi) Without Slots	Gain (dBi) With Slots
3 GHz	3	3.4
4 GHz	4.1	6.8
5 GHz	7.4	7.9
6 GHz	8.5	9.3
7 GHz	9.2	10.8
8 GHz	9.1	10.4
9 GHz	9	11
10 GHz	8.2	10.5

4 Antenna Prototyping and Measurement

Fig. 6 illustrates the fabricated model of the SL-AVA antenna, showing both the front and back sights of the structure. The antenna was manufactured using Rogers RT/Duroid 5880 substrate material, which possesses a relative dielectric constant (ε_r) of 2.2 and a substrate thickness of 1.58 mm. The precision in substrate selection is crucial for achieving the desired electromagnetic performance, particularly in UWB applications. For the experimental validation, the antenna's scattering parameters were measured using a Rohde & Schwarz ZNB20 Vector Network Analyzer (VNA). The combination of high-performance substrate and accurate measurement setup ensures the reliability and repeatability of the observed results, thereby facilitating a comprehensive understanding of the antenna’s structural and electromagnetic characteristics.

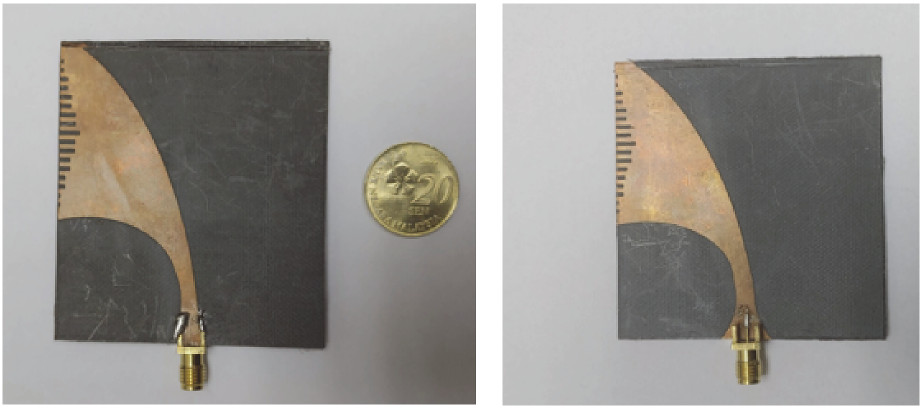

(a) (b)

Fig. 6 – *Fabricated SL-AVA prototype*: (a) *Front*; (b) *Back.*

Fig. 7 illustrates a comparative analysis of the simulated and measured reflection coefficients (S_{11}) for the designed SL-AVA antenna across the UWB frequency spectrum. S_{11} represents the fraction of incident energy reflected at the antenna's feed point due to impedance discrepancies. A value below -10 dB is typically considered acceptable, signifying that over 90% of the power is transferred efficiently with minimal reflection. As shown in the graph, both the simulated and measured S_{11} values remain consistently below the -10 dB threshold throughout the entire UWB range. This high degree of agreement between simulation and measurement confirms the antenna’s effective impedance matching and validates the accuracy of the design methodology. Moreover, the broad impedance bandwidth achieved by the antenna underpins its suitability for UWB applications, where consistent operation across a broad frequency spectrum is essential for dependable and high-speed wireless connectivity.

Fig. 8 presents a comparative plot of the simulated and measured Voltage Standing Wave Ratio (VSWR) of the SL-AVA antenna across the UWB frequency band. VSWR is a critical parameter that assesses the efficacy of power handover between the antenna and its feed network by quantifying the extent of impedance matching. A lower VSWR indicates reduced reflections and better impedance alignment, with a value below 2 typically considered acceptable for practical antenna systems. It can be seen from the figure that the simulated and measured VSWR consistently fall below the critical value of 2 over the entire UWB spectrum. This strong correlation between simulated and experimental results confirms that the proposed antenna maintains excellent impedance matching over the designated bandwidth. Consequently, the antenna demonstrates low reflection losses and efficient energy transfer, making it well-matched for ultra-wideband applications.

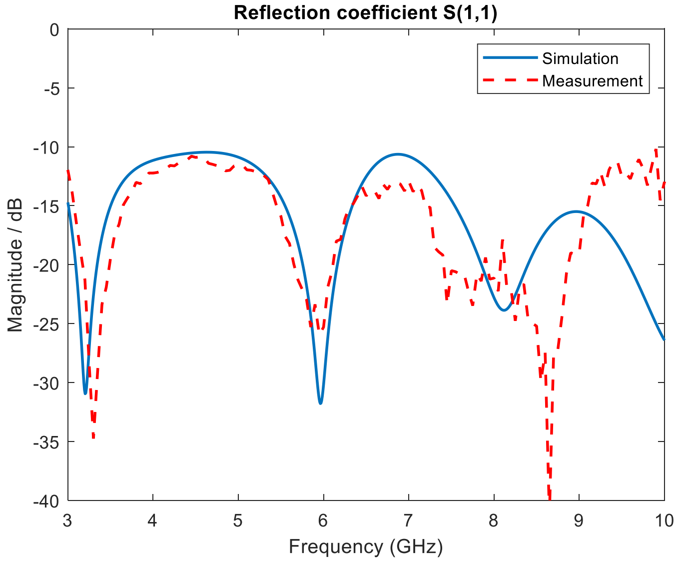

Fig. 7 – *Measured and simulated* (S_{11}).

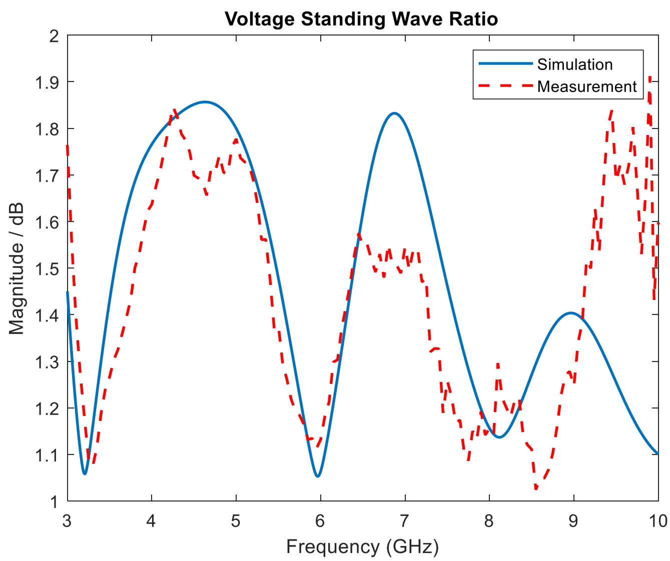

Fig. 8 – *Measured and simulated VSWR.*

4.1 Comparison of antenna performance

A detailed comparison between the proposed SL-AVA antenna and previously reported UWB antennas is provided in **Table 3,** focusing on several key performance indicators, including operational bandwidth, substrate material, antenna dimensions, realized gain, and application relevance.

Table 3

A comparison is made between the performance of the proposed antenna and that of existing designs in previous research.

Reference	Material	Peak Gain (dBi)	Frequency (GHz)	Dimensions	Application
[4]	FR4	9.2	1.85-9.2	0.734λ × 0.432λ	Through wall Imaging (TWI)
[15]	FR4	9.6	2.5-11.3	1.07λ×0.58λ	Through-the-wall radar imaging (TWRI)
[16]	Rogers RO3003	8.5	3.99 -12.28	1.81λ×0.88λ	Radar sensing system
[17]	FR4	8.2	1.9 -12	1.07λ×0.58λ	Through-the-wall radar (TWR)
[18]	FR4	7.66	1-4	0.303λ×0.36λ	See through the wall
Proposed	Rogers 5880	11	3-10	0.661λ×0.605λ	Through-the-wall radar imaging (TWRI)

The proposed design demonstrates several significant improvements over the referenced antennas [4, 16 – 19]. It offers an extensive frequency coverage across the entire UWB spectrum, ensuring broad operational capability. The antenna exhibits a high gain, which enhances signal transmission and reception performance. Furthermore, it achieves a wide impedance bandwidth, defined by a reflection coefficient ($|S_{11}|$) less than or equal to -10 dB, indicating efficient impedance matching and minimal signal reflection. One of the most distinguishing features of the proposed antenna is its compact physical footprint, which is notably smaller than that of comparable designs. This compactness, combined with superior electrical characteristics, makes the antenna highly suitable for integration into space constrained UWB systems and modern wireless communication platforms.

5 Conclusion

The development of a slot-loaded antipodal Vivaldi antenna (SL-AVA) for TWRI has been successfully presented in this work. Strategic incorporation of rectangular slots on the flares significantly enhances the antenna’s effective aperture while suppressing surface wave propagation. As a result, the antenna achieves key performance metrics including a wide impedance bandwidth ($|S_{11}|$

< -10 dB), low VSWR (< 2), high directional gain, and consistent radiation behavior in both E- and H-planes. Fabrication and experimental validation confirm strong agreement with simulations, reinforcing the reliability and practicality of the design. The compact form factor, coupled with its directive radiation and broadband performance, makes the SL-AVA an ideal candidate for TWRI systems. Beyond TWRI, its characteristics also render it suitable for applications in security surveillance, non-destructive testing, and remote sensing technologies, demonstrating the antenna's versatility and real-world relevance.

7 References

[1] K. Mu, T. H. Luan, L. Zhu, L. X. Cai, L. Gao: A Survey of Handy See-Through Wall Technology, IEEE Access, Vol. 8, April 2020, pp. 82951 – 82971.

[2] A. Wang, C. Chen, W. Chen: Cluster Adaptive Matching Pursuit for Multipolarization Through-Wall Radar Imaging, IEEE Sensors Journal, Vol. 23, No. 1, January 2023, pp. 414 – 424.

[3] E. J. Baranoski: Through-Wall Imaging: Historical Perspective and Future Directions, Journal of the Franklin Institute, Vol. 345, No. 6, September 2008, pp. 556 – 569.

[4] Y. Rai, S. Gotra, B. Kumar, S. Agarwal, D. Singh: A Compact Ultrawideband Antipodal Vivaldi Antenna and Its Efficacy in Through-Wall Imaging, Sensing and Imaging, Vol. 25, No. 1, December 2024, p. 12.

[5] K. Raha, K. P. Ray: Through Wall Imaging Radar Antenna with a Focus on Opening New Research Avenues, Defence Science Journal, Vol. 71, No. 5, September 2021, pp. 670 – 681.

[6] S. Ahmed, A. Joret, N. Katiran, M. F. Liew Abdullah, Z. Zakaria, M. S. Sulong, A. F. Osman: Design of UWB Antipodal Vivaldi Antenna with Rectangular Corrugated Edges for Through Wall Imaging (TWI) Applications, AIP Conference Proceedings, Vol. 2998, No. 1, March 2024, p. 040007.

[7] J. Wang, J. Liu, K. Hou, Y. Li: A Novel Antipodal Vivaldi Antenna for Ultra-Wideband Far-Field Detection, AEU - International Journal of Electronics and Communications, Vol. 164, May 2023, p. 154626.

[8] S. Ahmed, A. Joret, N. Katiran, M. F. Liew Abdullah, Z. Zakaria, M. S. Sulong: Ultra-Wideband Antipodal Vivaldi Antenna Design Using Target Detection Algorithm for Detection Application, Bulletin of Electrical Engineering and Informatics, Vol. 12, No. 4, August 2023, pp. 2165 – 2172.

[9] J. G. Vera-Dimas, M. Tecpoyotl-Torres, V. Grimalsky, S. V. Koshevaya, M. Torres-Cisneros: Analysis of Equivalent Antennas in RT Duroid 5880 and 5870 for GPS Operation Frequency, Proceedings of the IEEE Electronics, Robotics and Automotive Mechanics Conference, Cuernavaca, Mexico, September 2010, pp. 754 – 758.

[10] C. B. Hien, H. Shirai, D. N. Chien: Analysis and Design of Antipodal Vivaldi Antenna for UWB Applications, Proceedings of the 5th International Conference on Communications and Electronics (ICCE), Danang, Vietnam, July 2014, pp. 39 – 394.

[11] K. A. Reddy, S. Natarajamani, S. K. Behera: Antipodal Vivaldi Antenna UWB Antenna with 5.5 GHz Band-Notch Characteristics, Proceedings of the International Conference on Computing, Electronics and Electrical Technologies (ICCEET), Nagercoil, India, March 2012, pp. 821 – 824.

[12] S. Ahmed, A. Joret, N. Katiran, M. I. Abbasi, F. S. Khan: An Improved Design of UWB Slotted Antipodal Vivaldi Antenna for Through-wall Imaging (TWI) Systems Period. Polytech. Electr. Eng. Comput. Sci., Vol. 69, No. 2 , 2025 pp. 207 – 214.

[13] A. S. Dixit, S. Kumar: A Survey of Performance Enhancement Techniques of Antipodal Vivaldi Antenna, IEEE Access, Vol. 8, February 2020, pp. 45774 – 45796.

[14] K. Çelik: A Novel Asymmetric Antipodal Vivaldi MIMO Antenna, AEU - International Journal of Electronics and Communications, Vol. 187, December 2024, p. 155529.

[15] B. Dursun: The Novel Antipodal Vivaldi Antenna with Improved Gain, Transactions on Electromagnetic Spectrum, Vol. 4, No. 1, January 2025, pp. 1 – 6.

[16] R. R. Menon, S. Najeeb, S. N. Prabhu, T. A. George, A. Kuriakose, S. K. Diwakaran: An Improved Vivaldi Antenna Design for Through-Wall Radar Imaging, Proceedings of the International Conference on Communication and Electronics Systems (ICCES), Coimbatore, India, July 2019, pp. 1096 – 1100.

[17] X. Shao, L. Deng, C. Zhou, T. Yan, C. Tang, X. Gao, L.- L. Qiu: Broadband Antipodal Vivaldi Antenna with Simultaneous Flat Gain and Filtering Characteristic, Arabian Journal for Science and Engineering, Vol. 48, No. 5, May 2023, pp. 6831 – 6839.

[18] A. Kuriakose, T. A. George, S. Anand: Improved High Gain Vivaldi Antenna Design for Through-Wall Radar Applications, Proceedings of the International Symposium on Antennas & Propagation (APSYM), Cochin, India, December 2020, pp. 58 – 61.

[19] V. P. Cam, S. Van Tran, D. B. Nguyen: An Array of Antipodal Vivaldi Antenna with Genetic Optimization, Proceedings of the International Conference on Advanced Technologies for Communications (ATC), Ho Chi Minh City, Vietnam, October 2018, pp. 142 – 145.